

Non-Gaussianity Unleashed

Jonathan S. Horner and Carlo R. Contaldi

Theoretical Physics, Blackett Laboratory, Imperial College, London, SW7 2BZ, UK

The Hamilton-Jacobi (HJ) approach for exploring inflationary trajectories is employed in the generation of generalised inflationary non-Gaussian signals arising from single field inflation. Scale dependent solutions for f_{NL} are determined via the numerical integration of the three-point function in the curvature perturbation. This allows the full exploration of single field inflationary dynamics in the out-of-slow-roll regime and opens up the possibility of using future observations of non-Gaussianity to constrain the inflationary potential using model-independent methods. The distribution of ‘equilateral’ f_{NL} arising from single field inflation with both canonical and non-canonical kinetic terms are shown as an example of the application of this procedure.

Density perturbations due to primordial, Gaussian scalar metric perturbations are a very good fit to the observed structure in the Universe. The simplest model for seeding the initial, super-horizon curvature fluctuations required in this picture is one where small perturbations in a single inflaton field ϕ freeze out on large scales during the phase of quasi-de Sitter expansion. The perturbations are expected to be very close to Gaussian.

It is difficult to distinguish between different inflation models if only scalar perturbations are measured. However if the non-Gaussian contribution from higher order effects could be characterised it would allow the breaking of the slow-roll degeneracy and resolve detailed information about the shape of the inflaton potential $V(\phi)$ and in principle allow the constraining of more complicated forms of the action for ϕ .

Over the past decade much work has gone into the quantitative prediction of non-Gaussianity in both single field [1], multi-field models (see [2] for a review) and ones with non-canonical forms for the action. The formalism extends the calculation of the two-point function in the gauge invariant curvature perturbation ζ to third order. The two-point function, in the Fourier expanded perturbation $\zeta(\mathbf{k})$, defines the second moment of the distribution of the perturbations via an isotropic power spectrum $\langle \zeta(\mathbf{k}_1)\zeta^*(\mathbf{k}_2) \rangle = (2\pi)^3 \delta^{(3)}(\mathbf{k}_1 + \mathbf{k}_2) P(k_1)$. The three-point function vanishes in the Gaussian case and is defined via an f_{NL} amplitude [1]

$$\langle \zeta(\mathbf{k}_1)\zeta(\mathbf{k}_2)\zeta(\mathbf{k}_3) \rangle = \frac{6}{5}(2\pi)^3 \delta^{(3)}(\mathbf{k}_1 + \mathbf{k}_2 + \mathbf{k}_3) \times \quad (1)$$

$$f_{\text{NL}}(k_1, k_2, k_3) (P_{k_1} P_{k_2} + 2 \text{ perms}) .$$

Analytical studies of the prediction for f_{NL} have focused on particular configurations of the triangle $\mathbf{k}_1 + \mathbf{k}_2 + \mathbf{k}_3$ (‘equilateral’ $k_1 = k_2 = k_3$, ‘squeezed’ $k_1 \ll k_2, k_3$, etc.) and on specific models of inflation. The ‘squeezed’ signal from single field inflation obeys a consistency relation that means it is always small $f_{\text{NL}} \ll 1$, including in the non slow-roll limit [3]. This level of non-Gaussianity presents an observational challenge for even the most optimistic future survey forecasts. Large levels of f_{NL} are instead predicted in e.g. the equilateral limits in single

field models in the out-of-slow-roll limit or with non-canonical kinetic terms where the speed of sound c_s for the inflaton can be less than unity with respect to the speed of light [4–6], DBI type models [7], and models with multiple fields that undergo large accelerations [8].

A number of authors have examined the numerical prediction in out-of-slow-roll models that result in large f_{NL} [9, 10]. These have focused on ad-hoc modifications of the inflaton potential to induce temporary variations in the slow-roll parameters ϵ and/or η and have only been applied to specific cases. The subtleties involved in the numerical evaluation of the integrals required in the *in-in* calculation of the three-point function (1) were explored in [9, 10].

This *letter* introduces a generalised study of single field non-Gaussianity employing the HJ trajectory formalism [11]. This procedure allows for the calculation of f_{NL} arising from random trajectories and thus extends the HJ approach for constraining the shape of the inflationary potential to non-Gaussian observations. This type of analysis can complement the similar exploration involving tensor contributions from different inflationary trajectories. Two preliminary examples of these explorations are shown here; the first being an ensemble of single field inflation trajectories with a canonical kinetic term ($c_s = 1$) and the second being a case for $c_s \neq 1$. In both cases results for equilateral f_{NL} as a function of wavenumber k are presented. A more general study and discussion of the method will be reported in [12]. A choice of units such that that $M_{\text{pl}}^2 \equiv 1/8\pi G = 1$ and $c = 1$ is used throughout.

Hamilton-Jacobi formalism.— The HJ formalism [11, 13] allows for the exploration of all possible inflationary trajectories consistent with a single inflaton evolving monotonically in an FRW universe. The natural basis for labelling points in the phase-space of possible trajectories is an infinite series of ‘slow-roll’ co-ordinates that define the distance of any point along the trajectory from pure de Sitter evolution. These are defined as

$$\epsilon = 2 \left(\frac{H'(\phi)}{H(\phi)} \right)^2 \quad \text{and} \quad \lambda_l = 2^l \frac{(H')^{l-1}}{H^l} \frac{d^{(l+1)}H}{d\phi^{(l+1)}} , \quad (2)$$

where the value of the scalar field ϕ is used as an indepen-

dent parameter, H is the Hubble rate, and primes denote differentiation with respect to ϕ . Re-casting the Friedmann equations into a form where all quantities depend on ϕ one obtains

$$\frac{d\phi}{dt} = -2H'(\phi), \quad (3)$$

$$[H'(\phi)]^2 - \frac{3}{2}H(\phi)^2 = -\frac{1}{2}V(\phi), \quad (4)$$

where t is cosmological time and $V(\phi)$ is the inflaton potential. This allows one to define an infinite hierarchy of differential equations whose solutions self-consistently determine possible inflationary trajectories without the need to specify a potential $V(\phi)$

$$\frac{d\epsilon}{dN} = 2\epsilon(\epsilon - \eta), \quad (5)$$

$$\frac{d\lambda_l}{dN} = (l\epsilon - (l-1)\eta)\lambda_l - \lambda_{l+1}, \quad (6)$$

where $l = 0, 1, \dots$ and $\eta \equiv \lambda_1$, $\xi \equiv \lambda_2$ and the number of e -folds N , defined via $dN/dt = H$, has replaced t as the independent parameter by making use of the relation $d\phi/dN = -\sqrt{2\epsilon}$. The system (5)-(6), together with the differential equation $dH/dN = -H\epsilon$ can be integrated with random initial conditions to obtain a Monte Carlo sampling of inflationary trajectories [13]. The hierarchy can be truncated consistently by imposing that $\lambda_l = 0$ for all $l > l_{\max}$. The resulting solutions are exact but only cover a subset of all possible of solutions, limiting the structure and complexity of the trajectories.

Briefly, the scheme imposed here for Monte Carlo sampling of HJ trajectories is based on a ‘hierarchical prior’ defined as follows; the initial values of the parameters are $\epsilon = 1$, and the rest of the slow-roll parameters are randomly drawn from a uniform distribution with the ranges $[-0.1, 0.1]$ for η , and $[-0.1, 0.1] \times 10^{2-l}$ for λ_l , $l > 1$. The condition $\lambda_{l_{\max}} = 0$ is imposed. The choice for ϵ ensures that inflation ends for that trajectory at the point where the random boundary conditions are imposed. The system is then integrated back in time for total of number of e -folds N that is itself drawn from a uniform distribution with range [40, 80]. This completely fixes the inflationary model and, by construction, ensures inflation both ends and provides the necessary e -foldings compatible with observations. Other choices can be made for the priors used in drawing random boundary conditions and also in the location of the conditions along the trajectory and it should be noted that different choices will affect the final distributions in the observables.

Two-point function.— The trajectories define all background quantities that are required for computing the correlations of ζ on super-horizon scales arising from the period of inflation. To do this the late-time solution for ζ is obtained by integrating the Mukhanov–Sasaki equation [14, 15] arising from expanding the action for ζ to second order in the perturbations (with constant sound

speed c_s):

$$\frac{d^2\zeta_k}{dN^2} + (3 + \epsilon - 2\eta)\frac{d\zeta_k}{dN} + \frac{c_s^2 k^2}{a^2 H^2}\zeta_k = 0, \quad (7)$$

where $\zeta_k \equiv \zeta(\mathbf{k})$ and N is again used as the independent variable. Bunch–Davies initial conditions [16] are assumed for each ζ_k at sufficiently early times when $c_s k \gg aH$. The initial condition for H is chosen such that this condition holds at time $N = 0$. The system is integrated numerically for a range of k values up until the mode is sufficiently larger than the horizon (i.e. $c_s k \ll aH$) to ensure convergence of ζ_k to a constant.

The quantity $P_\zeta(k) = |\zeta_k|^2$, at a time when $c_s k \ll aH$ is then the power spectrum of primordial, super-horizon curvature perturbations that seeds structure formation. In the slow-roll regime, where $\lambda_l \ll 1$, the dimensionless power spectrum will approach a scale invariant solution $k^3 P_\zeta(k) \sim k^{n_s-1}$. The n_s for each trajectory is calculated using a second order finite difference scheme around a pivot point k_* . The first order slow-roll prediction is $n_s - 1 \approx 2\eta - 4\epsilon$ [17]. $P_\zeta(k)$ can then be compared to observations to constrain the possible set of solutions $\lambda_l(N)$ or equivalently $H(N)$ and/or $V(\phi)$. The latter being the fundamental property of interest in determining the nature of the inflaton.

Three-point function.— The inflationary trajectories can also be used to obtain generalised non-Gaussian predictions. The amplitude of the three-point correlation function for ζ can be obtained by considering the action for a perturbed, minimally coupled scalar field up to third order in the perturbation[1, 5, 6]

$$\begin{aligned} S = \int d^4x \frac{a^3 \epsilon}{c_s^2} \left[-\frac{2}{3H} \left(1 - \frac{1}{c_s^2} \right) \zeta^3 \right. \\ \left. + \frac{1}{c_s^2} (3(c_s^2 - 1) + \epsilon + 2\eta) \zeta \dot{\zeta}^2 + \frac{1}{a^2} (1 - c_s^2 + \epsilon) \zeta (\partial\zeta)^2 \right. \\ \left. - \frac{\epsilon}{a^2} (\epsilon - \eta) \zeta^2 \partial^2 \zeta - \frac{2\epsilon}{c_s^2} \left(1 - \frac{\epsilon}{4} \zeta \partial_i \zeta \partial_i \zeta \partial^{-2} \zeta \right) \right. \\ \left. + \frac{\epsilon^2}{4c_s^2} \partial^2 \zeta \partial_i \partial^{-2} \zeta \partial_i \partial^{-2} \zeta \right], \quad (8) \end{aligned}$$

where overdots denote differentiation with respect to t , $\partial_i \equiv \partial/\partial x_i$, and ∂^2 and ∂^{-2} are the Laplacian operator and its inverse. This action differs from ones usually presented in the literature in that no field redefinition has been introduced in order to avoid assumptions about boundary conditions that would lead to unphysical evolution of some of the terms for generalised trajectories i.e. ones where $\eta_V = 2(\epsilon - \eta)$ is still evolving when ζ_k is outside the horizon. This will be elaborated on in [12]. The three-point function at the end of inflation with $N = N_e$ can be computed in the interaction picture by integrating the interaction Hamiltonian in time [1, 6]

$$\begin{aligned} \langle \zeta_{k_1}(N_e) \zeta_{k_2}(N_e) \zeta_{k_3}(N_e) \rangle = \\ -i \int_{-\infty}^{N_e} dN \langle [\zeta_{k_1}(N_e) \zeta_{k_2}(N_e) \zeta_{k_3}(N_e), H_{\text{int}}(N)] \rangle, \quad (9) \end{aligned}$$

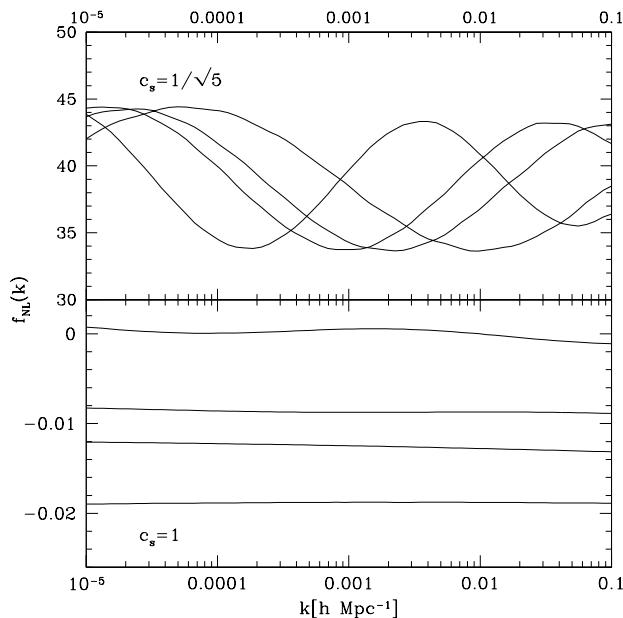


FIG. 1. A selection of $f_{\text{NL}}(k)$ spectra arising from typical trajectories for two cases; constant $c_s = 1$ (bottom) and $c_s = 1/\sqrt{5}$ (top). The f_{NL} in the $c_s \neq 1$ exhibits strong scale dependence whereas for $c_s = 1$ it is more mild.

where H_{int} is the Hamiltonian for the three-point function arising from (8).

This calculation can be carried out analytically in the slow-roll regime [1, 6] and in the out of slow-roll picture and/or non-canonical field case if the slow-roll parameters are constant [5, 18]. When considering the out of slow-roll case with general, non-stationary trajectories the calculation must necessarily be carried out numerically. A numerical calculation of the integrals involved in (9) has been carried out for specific inflation models with features in the potential [9, 10]. Here (9) is integrated numerically for each Monte Carlo trajectory [19]. The equilateral case of $k_1 = k_2 = k_3 \equiv k$ is chosen in what follows but the calculation is valid for all configurations. The aim in this case is to obtain the function $f_{\text{NL}}(k)$.

From equations (1) and (9), this can be re-cast as $f_{\text{NL}}(k) = 2 \text{Im}(z_k)$ where the complex mode z_k satisfies the following differential equation

$$\frac{dz_k}{dN} = \left(\frac{1}{\zeta_k^*} \frac{d\zeta_k^*}{dN} - \frac{2}{\zeta_k} \frac{d\zeta_k}{dN} \right) z_k + f_1 \frac{\zeta_k^*}{\zeta_k^2} \left(\frac{d\zeta_k}{dN} \right)^3 + f_2 |\zeta_k|^2 + f_3 \frac{\zeta_k^*}{\zeta_k} \left(\frac{d\zeta_k}{dN} \right)^2, \quad (10)$$

with initial condition $z_k \rightarrow 0$ as $N \rightarrow -\infty$ and f_i are

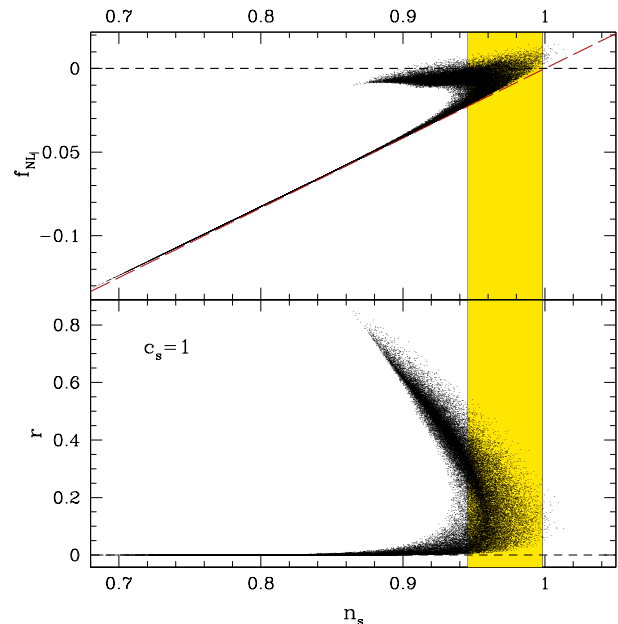


FIG. 2. The values of the tensor-to-scalar ratio r (bottom) and f_{NL} (top) plotted against the scalar spectral index n_s . All quantities are obtained from the numerical spectra at a single pivot scale. Some 10^4 trajectories were included in the ensemble with $c_s = 1$. The shaded area shows the 95% confidence region for n_s allowed by the WMAP 9-year results [20]. The red (dashed) line shows $f_{\text{NL}} \sim 5(n_s - 1)/12$ attractor expected in the slow-roll regime for equilateral f_{NL} .

defined as

$$\begin{aligned} f_1 &= \frac{10Ha^3\epsilon}{9c_s^2} \left(1 - \frac{1}{c_s^2} \right), \\ f_2 &= -\frac{5k^2 a\epsilon}{6Hc_s^2} (c_s^2 - 1 + \epsilon - 2\eta), \\ f_3 &= -\frac{5Ha^3\epsilon}{6c_s^4} \left(6(c_s^2 - 1) + 4\eta + \frac{3\epsilon^2}{4} \right). \end{aligned} \quad (11)$$

The numerical integration of the system requires some care due to the highly oscillatory nature of the integrand at early times and the evolution of slow-roll parameters throughout the integration. Convergence of the integrals with respect to both early and late time contributions has been verified [12].

Two examples of the results obtained from the numerical procedure discussed above are reported here. The first is an ensemble of $\mathcal{O}(10^5)$ trajectories with canonical speed of sound $c_s = 1$. The second is for a case where $c_s \neq 1$. For simplicity a constant value $c_s = 1/\sqrt{5}$ is chosen. From a Lagrangian perspective this corresponds to changing the coefficient and power of the kinetic term to functions of c_s^2 . To include c_s evolution an extra set of slow-roll parameters needs to be considered and consequently the functions f_i are more complicated.

The integration is carried out with the aid of GPU

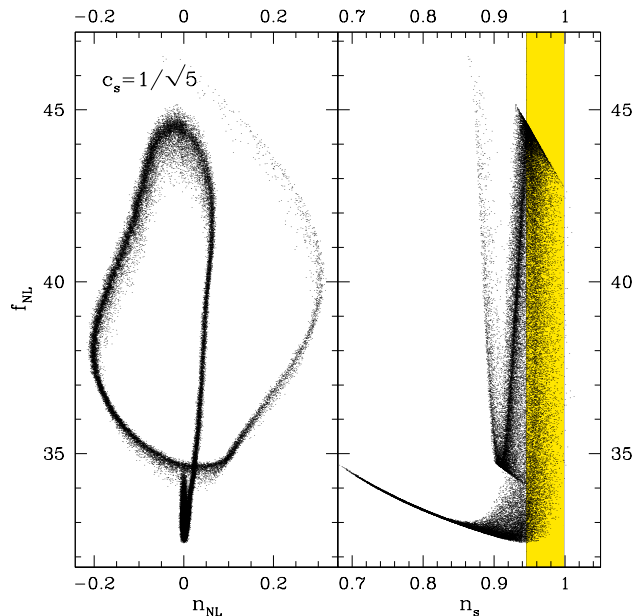


FIG. 3. f_{NL} plotted against n_s (right) and n_{NL} (left) for the same ‘slow-roll’ trajectories as in Fig. 2 but with constant $c_s = 1/\sqrt{5}$. The amplitude of the non-Gaussianity is much larger than for the $c_s = 1$ case. The complicated shape of the attractor is a consequence of the sinusoidal nature of $f_{\text{NL}}(k)$ which is not well approximated by a power law.

parallelisation and only requires on the order of a few minutes for the f_{NL} at all k samples to be computed for the entire ensemble. f_{NL} spectra resulting from typical trajectories with $n_s \approx 1$ for both ensembles are shown in Fig. 1. The amplitude of f_{NL} for the canonical case is small, in agreement with analytical estimates for single field inflation [1] and mild scale dependence is present in some of the solutions. The f_{NL} for the non-canonical case have a much higher amplitude, in agreement with analytical calculations [5] for the constant out-of-slow-roll case, and display a sinusoidal scale dependence in $\ln k$.

The phase portrait of the canonical ensemble is shown in Fig. 2 where the tensor-to-scalar ratio r and f_{NL} values are plotted against the n_s for each trajectory. The values shown are all obtained from the numerical spectra and are sampled at a fixed pivot scale k_* chosen to be to the largest mode in our sample corresponding to the scale of the horizon today.

The distribution of r is as expected with a clear slow-roll ‘attractor’, this is due to the fact that for the k_* corresponding to large scales today the spectra are sampled early on in the inflationary trajectories where the slow-roll parameters are typically small given our choice of hierarchical priors at the end of inflation. A more complex picture may arise from a wider prior, increasing l_{max} or for a choice of boundary conditions at the start

of inflation. The results also show a clear attractor in the value of $f_{\text{NL}}(k_*)$ that agrees with the slow-roll limit relation $f_{\text{NL}} \sim \frac{5}{12}(n_s - 1)$ for the equilateral case [1].

The phase picture for the non-canonical case is shown in Fig. 3. The amplitude of f_{NL} at the pivot point is plotted against n_s and the spectral tilt of f_{NL} defined as $n_{\text{NL}} = d \ln |f_{\text{NL}}| / d \ln k$ at the pivot scale. The attractor in this case displays a complicated structure. This is due to the fact that, for trajectories that result in near scale invariant scalar power spectra, f_{NL} is strongly scale dependent and is not well described by a power law amplitude and index [21]. A better parametrisation of f_{NL} in this case may be of the form $f_{\text{NL}}(k) = f_{\text{NL}}^0(1 + g \sin(\omega \ln k))$. Observations from *Planck* and other future surveys should be able to constrain the amplitudes of f_{NL} seen in this case [22] and potentially detect any scale dependence of the type seen in these solutions.

These results show that it is possible to compute f_{NL} for thousands of single field inflation models along with the usual n_s and r . The method agrees with the expected results of f_{NL} for canonical single field slow-roll inflation, i.e. small and probably unobservable. However, allowing non-canonical c_s generally results in observable levels of f_{NL} with significant scale dependence. Allowing for more structure and widening priors used in sampling the trajectories may also result in an extended range of amplitudes for f_{NL} . The method will be useful for constraining general single field inflation potentials and/or Lagrangian densities (see e.g. [23–25]). Further work will explore the landscape of models and, in particular, extend the approach to different ‘shapes’ or configurations for k_1 , k_2 , and k_3 and make detailed comparisons to observations.

Johannes Noller is acknowledged for useful discussions. This research is supported by an STFC student grant ST/F007027/1 and Consolidated grant ST/J000353/1.

-
- [1] J. M. Maldacena, JHEP **0305**, 013 (2003), arXiv:astro-ph/0210603 [astro-ph].
 - [2] N. Bartolo, E. Komatsu, S. Matarrese, and A. Riotto, Phys. Rept. **402**, 103 (2004), arXiv:astro-ph/0406398.
 - [3] P. Creminelli and M. Zaldarriaga, JCAP **0410**, 006 (2004), arXiv:astro-ph/0407059 [astro-ph].
 - [4] K. Tzirakis and W. H. Kinney, JCAP **0901**, 028 (2009), arXiv:0810.0270 [astro-ph].
 - [5] J. Noller and J. Magueijo, Phys.Rev. **D83**, 103511 (2011), arXiv:1102.0275 [astro-ph.CO].
 - [6] D. Seery and J. E. Lidsey, JCAP **0509**, 011 (2005), arXiv:astro-ph/0506056 [astro-ph].
 - [7] E. Silverstein and D. Tong, Phys.Rev. **D70**, 103505 (2004), arXiv:hep-th/0310221 [hep-th].
 - [8] D. Wands, Lect.Notes Phys. **738**, 275 (2008), arXiv:astro-ph/0702187 [ASTRO-PH].
 - [9] X. Chen, R. Easther, and E. A. Lim, JCAP **0706**, 023

- (2007), arXiv:astro-ph/0611645 [astro-ph].
- [10] X. Chen, R. Easther, and E. A. Lim, JCAP **0804**, 010 (2008), arXiv:0801.3295 [astro-ph].
- [11] D. S. Salopek and J. R. Bond, Phys. Rev. D **42**, 3936 (1990).
- [12] J. Horner and C. R. Contaldi, In preparation.
- [13] R. Easther and W. H. Kinney, Phys.Rev. **D67**, 043511 (2003), arXiv:astro-ph/0210345 [astro-ph].
- [14] V. F. Mukhanov, JETP Lett. **41**, 493 (1985).
- [15] M. Sasaki, Prog.Theor.Phys. **76**, 1036 (1986).
- [16] T. Bunch and P. Davies, Proc.Roy.Soc.Lond. **A360**, 117 (1978).
- [17] E. D. Stewart and D. H. Lyth, Phys.Lett. **B302**, 171 (1993), arXiv:gr-qc/9302019 [gr-qc].
- [18] R. H. Ribeiro, JCAP **1205**, 037 (2012), arXiv:1202.4453 [astro-ph.CO].
- [19] A detailed review of the numerical integration and the subtleties it involves will be given in [12].
- [20] G. Hinshaw, D. Larson, E. Komatsu, D. Spergel, C. Bennett, *et al.*, (2012), arXiv:1212.5226 [astro-ph.CO].
- [21] The fact that the f_{NL} vs n_{NL} portrait resembles the greek letter ϕ appears to be entirely coincidental.
- [22] C. Burigana, C. Destri, H. de Vega, A. Gruppuso, N. Mandolesi, *et al.*, Astrophys.J. **724**, 588 (2010), arXiv:1003.6108 [astro-ph.CO].
- [23] H. V. Peiris, E. Komatsu, L. Verde, D. N. Spergel, C. L. Bennett, M. Halpern, G. Hinshaw, N. Jarosik, A. Kogut, M. Limon, S. S. Meyer, L. Page, G. S. Tucker, E. Wollack, and E. L. Wright, Astrophys.J. **148**, 213 (2003), arXiv:astro-ph/0302225.
- [24] J. Lesgourgues, A. A. Starobinsky, and W. Valkenburg, JCAP **1**, 010 (2008), arXiv:0710.1630.
- [25] R. Bean, D. J. Chung, and G. Geshnizjani, Phys.Rev. **D78**, 023517 (2008), arXiv:0801.0742 [astro-ph].